RSC Advances

ROYAL SOCIETY OF CHEMISTRY

www.rsc.org/advances

Journal Name

RSCPublishing

ARTICLE

The role of intermolecular interactions involving halogens in the supramolecular architecture of a series of Mn(II) coordination compounds

Cite this: DOI: 10.1039/x0xx00000x

Hamid Reza Khavasi*, Alireza Ghanbarpour and Alireza Azhdari Tehrani

Received 00th January ????.,
Accepted 00th January ????

DOI: 10.1039/x0xx00000x

www.rsc.org/

A series of four new manganese(II) complexes based on the $L^{4\text{-}X}$ ligand, where L is *N*-(4-halo)phenyl picolinamide ligands, synthesized, characterized and their supramolecular crystal structures were studied by geometrical analysis and theoretical calculation. Our study reveals the role of weak intermolecular interactions involving halogens, such as C-H•••X hydrogen bonds (in the cases of 1 and 2) and C-X•••X´-M halogen bonds (in the cases of 3 and 4), in the structural changes of supramolecular assemblies of coordination compounds. This study could provide further insight into discovering the role of weak intermolecular interactions in the context of metallosupramolecular assembly.

Introduction

In recent years, supramolecular assembly of coordination compounds has been attracting increasing attention, owing to their potential as functional materials.[1] In this regard, supramolecular chemists and crystal engineers have attempted to understand the rules of supramolecular assembly of metal-containing compounds by studying the solid-state structures of these systems. The results of these studies led to the recognition and elucidation of the role of different intermolecular interactions, such as secondary bonding, hydrogen and halogen bonds in metallosupramolecular self-assemblies.[2] Halogen bonding, an interaction between a halogen atom (Lewis acid, XB donor) and a donor of electron density (Lewis base, XB acceptor), has been now recognized as a reliable supramolecular tool in molecular self-assembly.[3] While halogen bonding has been well studied in organic systems, the progress in utilizing this type of intermolecular interaction to construct metallosupramolecular assemblies is still relatively unexplored.[4] In the context of metallosupramolecular assembly, C-X···X´-M halogen bonds has been identified as a supramolecular synthon in crystal design.[5] Also, it has been revealed that the electrostatic differences between organic (C–X) and inorganic (M–X′) halogens are responsible for distinct features of C–X···X′–M halogen bonding synthon.[6] It is obvious that such as understanding could be valuable to chemists in the tailoring of physical/chemical properties of materials.

In continuation of our research program aiming at the understanding of the role of intermolecular interactions in the metal-containing crystal structures,[7] a series of *N*-(4-halo)phenyl picolinamide ligands, $L^{4\text{-F}}$, $L^{4\text{-Cl}}$, $L^{4\text{-Br}}$ and $L^{4\text{-I}}$, in which the halogen atom is in the phenyl *para* position, have been employed for the synthesis of four new Mn(II) complexes. The geometrical analysis, Hirshfeld surface analysis and theoretical calculation reveal the importance of trifurcated hydrogen bonding interactions of the $_{amide}$N-H···Cl and C-H···Cl type and C–X···Cl–Mn halogen bonding synthon in the self-assembly of this series of complexes.

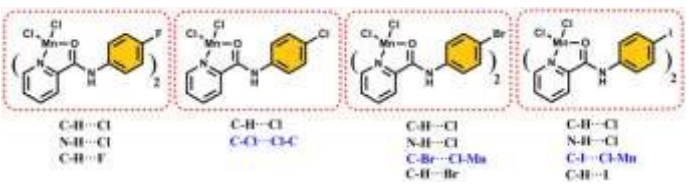

Scheme 1. A comparison between intermolecular interactions controlling the crystal packing arrangement of complexes **1**-**4**

Results and Discussion

Synthesis. The ligands, $L^{4\text{-F}}$, $L^{4\text{-Cl}}$, $L^{4\text{-Br}}$ and $L^{4\text{-I}}$, were prepared by simply mixing the same equivalents of *para*-haloaniline and 2-picolininc acid in pyridine in the presence of triphenyl phosphite. The reaction of equimolar amounts of these ligands and $MnCl_2.4H_2O$ in methanol gave the corresponding complexes. Slow evaporation of the solvent resulted in air-stable crystals of **1**–**4** after a few days. The crystallographic data for compounds **1**–**4** are listed in Table 1.

Structural analysis $MnCl_2$ complexes, $[MnCl_2(L^{4\text{-F}})_2]$ (1), $[MnCl_2(L^{4\text{-Cl}})]$ (2), $[MnCl_2(L^{4\text{-Br}})_2]$ (3) and $[MnCl_2(L^{4\text{-I}})_2]$ (4). X-ray crystallography analyses reveal that **1**, **2**, **3** and **4** crystallize in Orthorhombic *Aba2*, Monoclinic $P2_1/n$, Monoclinic $P2_1/c$ and Orthorhombic *Pbcn* space groups, respectively. ORTEP diagrams of complexes **1**-**4** drawn with 30% ellipsoid probability have been shown in Figure 1. The asymmetric unit of **1** contains a crystallographically independent *N*-(4-fluoro)phenyl picolinamide ligand ($L^{4\text{-F}}$) ligand, a Mn(II) ion and a chloride ion. The

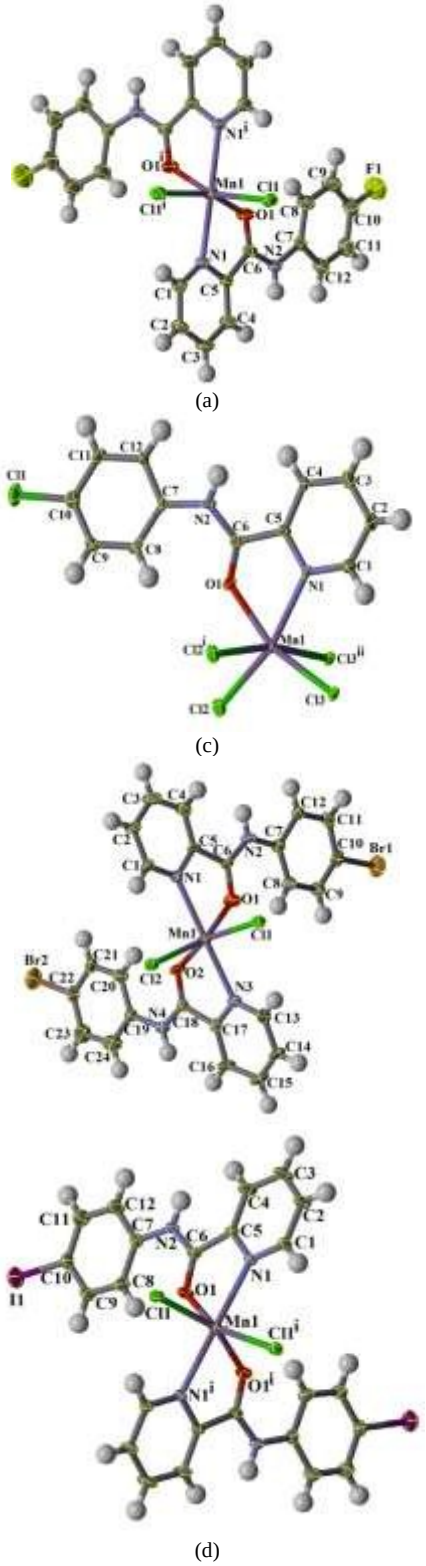

Figure 1. The ORTEP diagram of asymmetric unit of compounds **1** (a), **2** (b), **3** (c) and **4** (d). Ellipsoids are draw at 30% probability level. (a) i = 2-*x*,-*y*, *z*, (b) i = -*x*,1-*y*,2-*z* and ii= 1-*x*,1-*y*,2-*z* and (d) i=-*x*,*y*,1/2-*z* .

Table 1. Structural data and refinement parameters for complexes **1-4**.

	1	**2**	**3**	**4**
formula	$C_{24}H_{18}Cl_2F_2MnN_4O_2$	$C_{12}H_9Cl_3MnN_2O$	$C_{24}H_{18}Br_2Cl_2MnN_4O_2$	$C_{24}H_{18}Cl_2I_2MnN_4O_2$
fw	558.26	358.50	680.06	774.06
λ/Å	0.71073	0.71073	0.71073	0.71073
T/K	298(2)	298(2)	298(2)	298(2)
crystal system	Orthorhombic	Monoclinic	Monoclinic	Orthorhombic
space group	*Aba2*	$P2_1/n$	$P2_1/c$	*Pbcn*
a/Å	13.476(4)	6.8043(8)	20.474(9)	13.3390(12)
b/Å	19.011(4)	12.7288(13)	13.357(5)	9.4207(7)
c/Å	9.349(3)	15.384(2)	9.346(4)	20.8663(14)
β/°	90	94.851(11)	91.06(4)	90
V/Å^3	2394.9(12)	1327.7(3)	2555.3(19)	2622.1(4)
D_{calc}/Mg.m^{-3}	1.548	1.794	1.768	1.961
Z	4	4	4	4
μ (mm^{-1})	0.820	1.588	3.883	3.092
F(000)	1132	716	1340	1484
2θ (°)	56.00	54.00	58.70	52.00
R (int)	0.0985	0.1010	0.0914	0.0700
GOOF	1.011	0.914	0.863	1.072
R_1[a](I>2σ(I))	0.0461	0.0712	0.0790	0.0422
wR_2[b](I>2σ(I))	0.0746	0.0923	0.1754	0.0774
CCDC No.	1016027	1016026	1016023	1016022

[a] $R_1 = \Sigma||F_o| - |F_c||/\Sigma|F_o|$. [b] $wR_2 = [\Sigma(w(F_o^2 - F_c^2)^2)/\Sigma w(F_o^2)2]^{1/2}$.

coordination geometry around the Mn(II) ion can be described as a distorted octahedral, where the two bidentate $L^{4\text{-}F}$ ligands are bonded to the metal through neutral pyridine nitrogen and carbonyl oxygen atoms. The two remaining sites are occupied by two chloride ions. The two chloride ions are mutually *cis* to each other. In complex **1**, the Mn-N_{py} and Mn-O_{CO} bond distances are 2.315(3) and 2.224(3) Å, respectively and the O-Mn-N ligand bite angle is 70.55(11)°. Selected bond lengths and angles are summarized in Table 2. Figure 2 shows the crystal packing view of $[MnCl_2(L^{4\text{-}F})_2]$ in the *ab*-plane. In this crystal structure, each chloride ion acts as a trifurcated hydrogen-bond acceptor by forming $_{amide}$N-H···Cl and two C-H···Cl hydrogen bonds with pyridine and aryl hydrogen atoms of $L^{4\text{-}F}$ ligand. In the crystal packing of this complex, the fluorine atom of $L^{4\text{-}F}$ ligand is involved in C-H···F hydrogen bonds that are cooperated with the mentioned N-H···Cl and C-H···Cl hydrogen bonds to construct the final supramolecular structure. Parameters for selected hydrogen bonding interactions are collected in Table S1. Within the asymmetric unit of $[MnCl_2(L^{4\text{-}Cl})]$, **2**, there exist one Mn(II) ion, two chloride ions and a *N*-(4-chloro)phenyl picolinamide ligand ($L^{4\text{-}Cl}$) ligand. The Mn(II) is six-coordinate in a distorted octahedral geometry, coordinated by four bridging chloride ions and a chelating $L^{4\text{-}Cl}$ ligand (Mn-N_{py}=2.324(6) Å and Mn-O_{CO}=2.240(5) Å), with a bite angle of 71.0(2)°. Therefore, **2** is a one-dimensional coordination polymer built up from chloride-bridged Mn(II) edge-sharing octahedra extending along the *a*-axis, Figure 3. The Mn···Mn distance within the metal chain is 3.867(2) Å and the intrachain Mn···Mn···Mn angle is 125.90(4)°, which is comparable to those previously reported for $[MnCl_2(mapy)]$ (Mn···Mn= 3.6533(8) Å and ∠Mn···Mn···Mn=123.08(1)°) by Himmel and his co-workers.[8] As depicted in Figure 3, the supramolecular association between the 1D coordination polymers occurs through symmetrical halogen···halogen contacts, namely C10-Cl1···Cl1-C10 (Cl···Cl= 3.392(3) Å, ∠C-Cl···Cl=154.8(3)°). It is believed that this type of halogen-halogen contact caused by

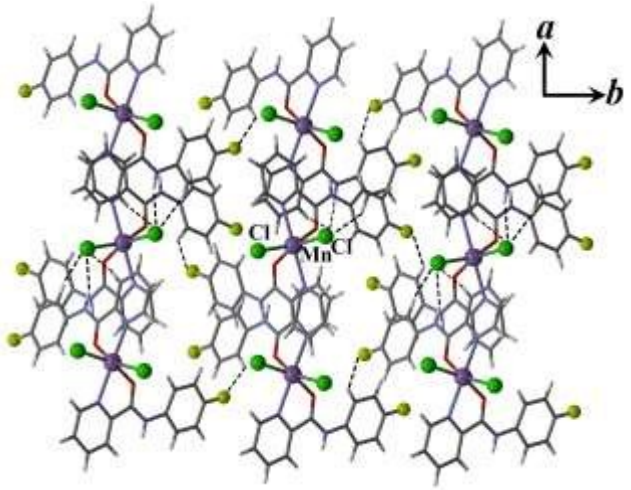

Figure 2. A side view representation of $[MnCl_2(L^{4\text{-}F})_2]$, **1,** showing the association of the adjacent discrete complexes through trifurcated hydrogen bonding interactions of the amideN-H•••Cl and C-H•••Cl type, in the *ab*-plane.

crystal packing effects and may therefore not necessarily represent an attractive contact.[9] As in this crystal structure, an inversion-generated intermolecular C10-Cl1···Cl1-C10 contact occurs, leading to association of coordination polymer chains in *ac*-plane. The 1D chain is further stabilized by C-H···Cl hydrogen bonding interactions, Figure 3 and Table S1.

In the asymmetric unit of $[MnCl_2(L^{4\text{-}Br})_2]$, **3**, there are two independent $L^{4\text{-}Br}$ ligands, two chloride ions and a Mn(II) ion, while in the asymmetric unit of $[MnCl_2(L^{4\text{-}I})_2]$, **4**, there are an independent *N*-(4-iodo)phenyl picolinamide ligand ($L^{4\text{-}I}$) ligand, a Mn(II) ion and a chloride ion. Complexes **3** and **4** present the same coordination sphere around the Mn(II) ion ie, two $L^{4\text{-}X}$ (X=Br for **3** and X=I for **4**) and two chloride ions, as described for **1**. The Mn-N_{py} bond distances are 2.302(8) and 2.323(8) Å for **3** and 2.305(4) Å for **4**, while the Mn-O_{CO} bond distances are 2.210(8) and 2.270(8) for **3** and 2.230(3) Å for **4**. The ligand O-Mn-N bite angles are 71.3(3)˚ and 71.10(11)˚ for **3** and **4**, respectively.

Similar to **1**, in the case of **3** and **4**, the chloride ions act as trifurcated hydrogen-bond acceptors by forming $_{amide}$N-H···Cl and two C-H···Cl hydrogen bonds with pyridine and aryl hydrogen atoms of $L^{4\text{-}X}$ (X=Br for **3** and X=I for **4**) ligand. As shown in figures 4 and 5, the carbon-bound bromine and iodine atoms are involved in C-X··· Cl-Mn halogen bonding interactions, namely C-Br··· Cl-Mn (Br··· Cl=3.599(3) Å and ∠C-Br··· Cl=175.3(4)˚) for **3** and C-I··· Cl-Mn (I··· Cl=3.585(1) Å and ∠C-I··· Cl=176.4(1)˚) for **4**, Table 3**.** Thus, the overall supramolecular architecture is constructed by linking neutral discrete $[MnCl_2(L^{4\text{-}Br/I})_2]$ complexes *via* a combination of hydrogen and halogen bonding interactions in the *ac*-plane.

The role of weak intermolecular interactions involving halogens in the assembly of a series of Mn(II) coordination complexes. One of the most prolific areas of current research in inorganic crystal engineering is aimed at understanding the intermolecular interactions (synthons) holding the three-dimensional arrays of metal-containing building blocks.[10] Among the intermolecular interactions, directional interactions like hydrogen and halogen bonding interactions are more interesting than non-directional intermolecular interactions, owing to their potential for designing predefined arrangements of molecular materials. Accordingly, in recent years there has been an interest in constructing metallosupramolecular assemblies based on hydrogen and halogen bonds.[11,5f,7d] Manganese plays an important role in many biological processes including water oxidation in photosystem II, dismutation of the superoxide anion radical (SOD process) and decomposition of hydrogen peroxide (catalase).[12] The amidic ligands are also particularly attractive not only because of their biological significance but also for their diversity in coordination modes.[13] As part of our research interest in both exploring the coordination chemistry of ligands containing amide functional group and metallosupramolecular chemistry focusing on understanding the intricacies of metal-containing crystal packing, we became interested in investigating how halogen substitution on the phenyl ring of amide-containing ligand might affect the crystal structure and possibly the coordination environment around the Mn(II) ion.[14] Reaction between 4-haloaniline and 2-picolininc acid

Table 2. Selected bond distances (Å) and angles (°) for complexes **1**-**4**.

		Complex			
		1	**2**	**3**	**4**
Bond distance	Mn1-N1	2.315(3)	2.324(6)	2.323(8)	2.305(4)
	Mn1-O1	2.224(3)	2.240(5)	2.270(8)	2.230(3)
	Mn1-Cl1	2.4627(12)	2.517(3)	2.453(3)	2.4669(13)
	Mn1-Cl2	-	2.561(2)	2.499(3)	-
	Mn1-N3	-	-	2.302(8)	-
	Mn1-O2	-	-	2.210(8)	-
Bond angle	N1-Mn1-O1	70.55(11)	70.98(19)	71.3(3)	71.10(11)
	N1-Mn1-Cl1	94.57(8)	161.10(14)	93.3(2)	92.75(9)
	O1-Mn1-Cl1	91.79(8)	90.61(15)	90.5(2)	91.18(9)
	N1-Mn1-Cl2	-	89.48(14)	88.9(2)	-
	O1-Mn1-Cl2	-	160.27(15)	156.9(2)	-
	N3-Mn1-O2	-	-	70.2(3)	-
	N3-Mn1-Cl1	-	-	90.0(2)	-
	O3-Mn1-Cl1	-	-	156.2(2)	-

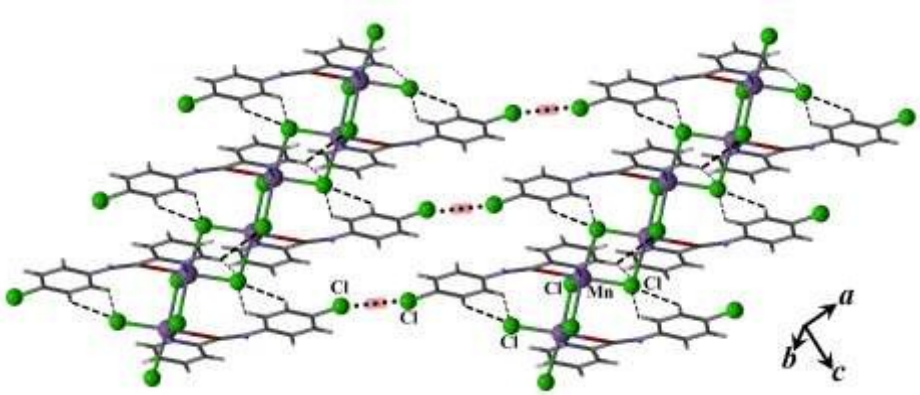

Figure 3. A side view representation of $[MnCl_2(L^{4\text{-}Cl})]$, **2,** showing the association of the one-dimensional coordination polymer chains through C-Cl•••Cl-C contacts, in ac-plane. The 1D chain is further stabilized by C-H•••Cl hydrogen bonding interactions, in the *ab*-plane.

give $L^{4\text{-}X}$ (X=F, Cl, Br and I) ligands, which is a good chelating ligand for Mn(II) ions. Thus, a series of Mn(II) coordination compounds, based on the *N*-(4-halo)phenyl picolinamide ligands, $L^{4\text{-}F}$, $L^{4\text{-}Cl}$, $L^{4\text{-}Br}$ and $L^{4\text{-}I}$ has been performed, in which non-covalent interactions involving halogen atoms, namely weak hydrogen and halogen bonds, could cooperate or compete with each other to direct the crystal packing architecture.

In these complexes, the coordination geometry of the Mn(II) ion is distorted octahedral due to the constraints represented by the tight bite angle of O-Mn-N. Except for **2**, the manganese coordination sphere is constructed from two chloride ions and two $L^{4\text{-}X}$ ligands, which are perpendicularly oriented relative to each other. A survey in Cambridge Structural Database (CSD) reveals that this coordination mode is retained for Mn(II) complexes based on *N*-(4-methyl)phenyl picolinamide ($L^{4\text{-methyl}}$)[13c] ligand and *N*-phenylpicolinamide ($L^{4\text{-H}}$)[13a] ligands. Interestingly, this is even retained in the crystal structure of Mn(II) complex with *N*-(3-chloro)phenyl picolinamide ($L^{3\text{-Cl}}$) ligand.[13d] Noteworhy, in compound **2**, adjacent manganese(II) ions are bridged by chloride ions to form a 1D linear chain structure, while compound $[MnCl_2(L^{3\text{-Cl}})_2]$ is a discrete mononuclear complex.[13d]

The dihedral angle between the planes of pyridine and aryl rings lies between 3.13˚ and 12.31˚ for Mn(II) complexes. In these complexes, the intramolecular C-H···O_{CO} hydrogen bonding interaction favor the coplanarity between two aromatic rings. Compared to the structure of free ligands, the Mn(II) complexes exhibit lesser coplanarity due to the elimination of the possibility of the formation of intramolecular N-H···N_{py} hydrogen bonding interaction.[7c]

A comparison between intermolecular contacts controlling the crystal packing of **1**–**4** is illustrated in Scheme 1. As described above, the common feature in the crystal packing of these complexes is that adjacent discrete neutral complexes tend to link to each other through trifurcated hydrogen bonding interactions of the $_{amide}$N-H···Cl and C-H···Cl type. It is to be noted that the strength of this trifurcated hydrogen bonding synthon is diminished on going from **1** to **3** and further to **4**, Table S1. The mentioned trifurcated hydrogen bonding synthon is preserved for $[MnCl_2(L^{4\text{-H}})_2]$, $[MnCl_2(L^{4\text{-methyl}})_2]$ and $[MnCl_2(L^{3\text{-Cl}})_2]$, while different crystal structure of **2** results in the weakening of this supramolecular synthon. Furthermore, the

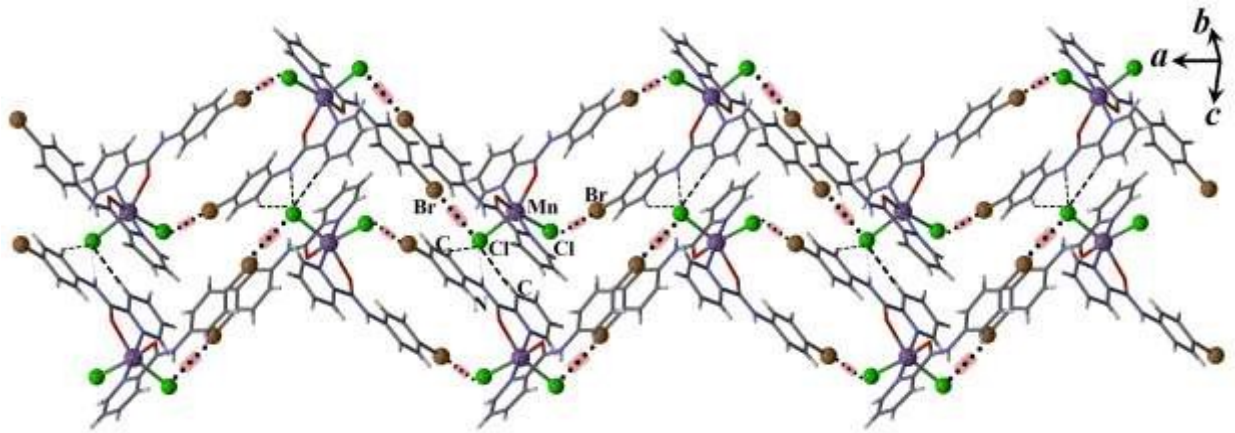

Figure 4. A side view representation of $[MnCl_2(L^{4\text{-Br}})_2]$, **3,** showing the association of the adjacent discrete complexes through trifurcated hydrogen bonding interactions of the amideN-H•••Cl and C-H•••Cl type and C-Br••• Cl-Mn halogen bonds, in the *ac*-plane. Halogen bonds are highlighted in red.

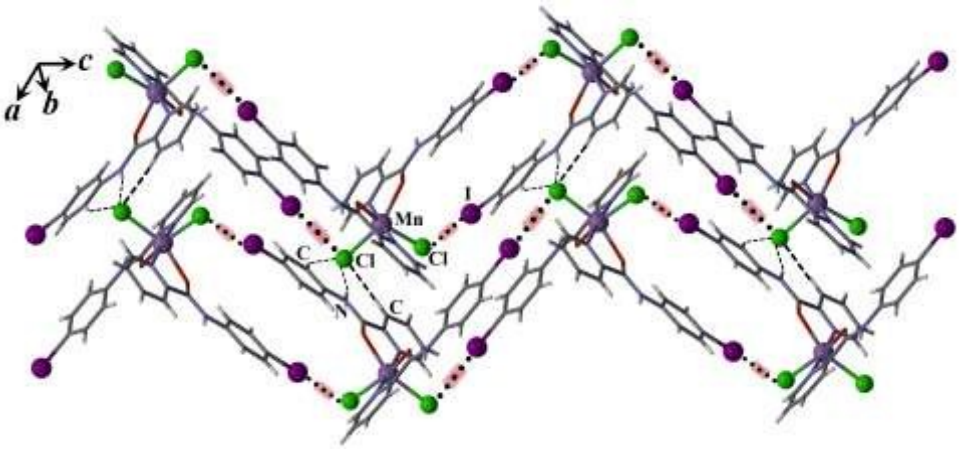

Figure 5. A side view representation of $[MnCl_2(L^{4\text{-}I})_2]$, **4,** showing the association of the adjacent discrete complexes through trifurcated hydrogen bonding interactions of the amideN-H•••Cl and C-H•••Cl type and C-I•••Cl-Mn halogen bonds, in the *ac*-plane. Halogen bonds are highlighted in red.

intermolecular contacts in the crystal structure of **1**-**4** are quantified *via* Hirshfeld surface analysis[15] using Crystal Explorer 3.0.[16] Hirshfeld surface analysis is a novel tool for the visualization and understanding of intermolecular interactions. A histogram of percentage contributions of different intermolecular interactions is shown in Figure 6, Table S2. In cases **2** and $[MnCl_2(L^{3\text{-}Cl})_2]$, these data reveal that there is a subtle interplay between metal coordination and intermolecular interactions. Noteworthy, when the chlorine substitution has been moved from *meta*- to *para*- position of the phenyl group of the ligand, the contribution percentages of H···H, C-H···π and Cl···π decreases, while π···π and C-H···O increases.[13d] However, changing the substitution position from *meta*- to *para*-position has no significant effect on the contribution of C-H···Cl to the Hirshfeld surface area. The histogram also indicates that upon the replacement of the phenyl group of *N*-phenylpicolinamide by *para*-halogen-substituted phenyl group, the probability of H···H, π···π and O···H decreases, while that of C-X···H, X···X and X···π increases. From **1** to **3** and further to **4**, the contribution of intermolecular interactions involving inorganic halogen atom decreases, while that of organic halogen atom increases. The results of Hirshfeld surface analysis also revealed that the lighter halogen atoms (fluorine and chlorine) are mainly involved in C-H···X hydrogen bonding interactions, while the heavier halogens (bromine and iodine) prefer halogen bonding interactions of the type C-X···Cl-Mn. Halogen···halogen interactions, which can be classified into two types depending on their geometries, ie type I (θ1=θ2) and type II (θ1≈180˚, θ2≈90˚). This intermolecular interaction is an important design element in the assembly of organic and metal-containing supramolecular structures.[3,4] Despite their weak nature, halogen-halogen interactions may often have the chance to play an important role in directing the supramolecular structure, even in the presence of strong intermolecular interactions such as hydrogen bonds.[4e-4l] It is now well-understood that for heavier halogen atoms the electron density is anisotropically distributed around the covalently bound halogen atoms. Accordingly, a region with a diminished electron density (σ-hole) is formed on the outermost portion of the halogen's surface along the extension of the C–X bond. The positive character of the σ-hole increases in going from the lighter to the heavier halogens, reflecting increasing polarizability.[17] This is the reason for the higher tendency of bromine and iodine to participate in halogen bonding interactions, as an electrophile (XB donor). Evidences for the electrophilic-nucleophilic nature of C–X···X′–M halogen bond and the nucleophilic role of inorganic halogen atom (M-X) in this interaction were provided by Brammer and his co-workers.[4c,4d]

Table **3**. Halogen Bonding geometries and calculated XB binding energies for Compounds **2**, **3** and **4**.

Complex	Interaction	C-X···X distance	C-X···X angle	Mn-X···X angle	Reduction of the sum of the VDW radii (%)	Symmetry code	Calculated binding energy
$[MnCl_2(L^{4\text{-}Cl})]$	C_{10}-Cl_1…Cl1-C_{10}	3.392(3)	154.8(3)	-	3.09	-2-x,1-y,1-z	-3.24
$[MnCl_2(L^{4\text{-}Br})_2]$	C_{10}-Br_1…Cl1-Mn1	3.599(3)	175.3(4)	92.27(9)	0.03	1-x,-y,1-z	-66.23
	C_{22}-Br_2…Cl2-Mn1	3.551(3)	174.9(4)	91.72(9)	1.37	2-x,-y,1-z	-66.63
$[MnCl_2(L^{4\text{-}I})_2]$	C_{10}-I_1…Cl1-Mn1	3.585(1)	176.4(1)	93.28(3)	9.47	-x,-y,-z	-78.26

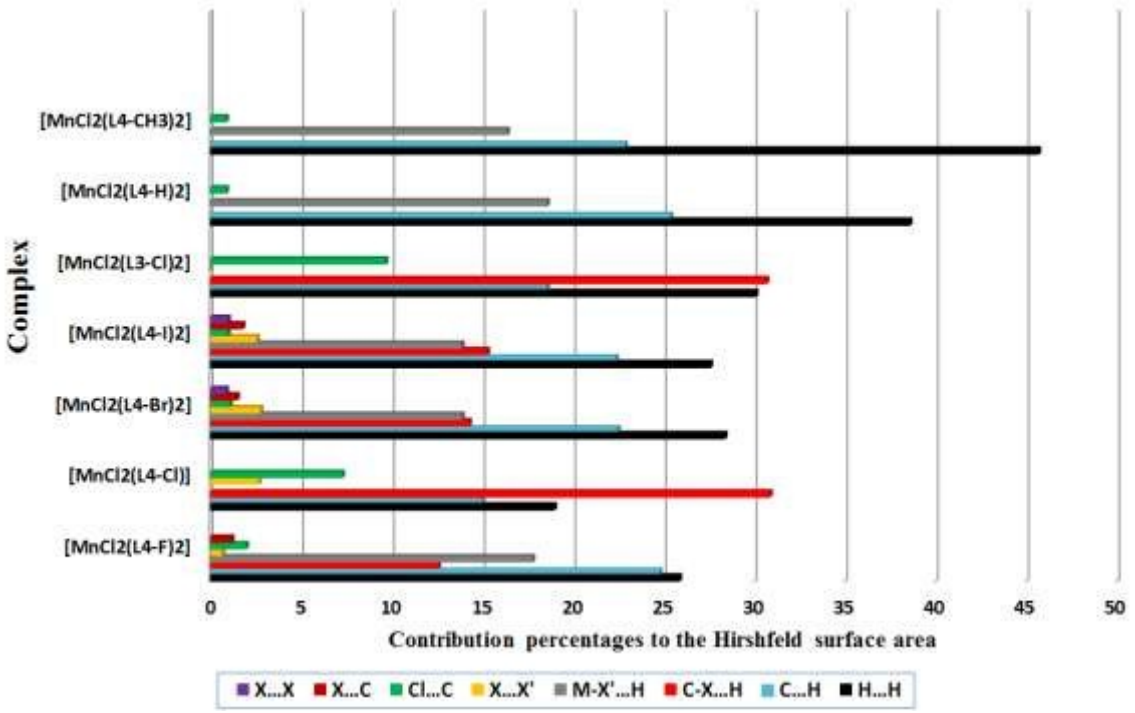

Figure 6. Relative contributions of various non-covalent contacts to the Hirshfeld surface area in complexes **1-4**, $[MnCl_2(L^{4\text{-}H})_2]$,[13a] $[MnCl_2(L^{4\text{-}Methyl})_2]$,[13c] and $[MnCl_2(L^{3\text{-}Cl})_2]$.[13d]

This can be rationalized by considering the alignment of the Mn–Cl group with the carbon bound bromine/iodine's σ-hole, Table 3. The C-X···Cl-Mn distances of 3.599(3) and 3.551(3) Å for **3** and 3.585(1) Å for **4** are 0.03%, 1.37% and 9.47%, respectively, shorter than sum of the van der Waals radii, Table 3. The nearly linear angle of C-X···Cl, 175.3(4)˚ and 174.9(4)˚ for X=Br and 176.4(1)˚ for X=I, is in agreement with the concept of electron donation into the sigma anti-bonding orbital of C-X bond.[18] The involvement of halogen atom in X···X′ and X···π interactions in **4**, in comparison to **3**, make up the slightly greater contribution (I···Cl=2.6% and I···π=1.8% for **4** and Br···Cl=2.8% and Br···π=1.5% for **3**), to the Hirshfeld surface area, Figure 6. The DFT calculations of the binding energy were performed on two relative fragments of coordination compounds **2-4**. As anticipated, the less attractive nature of C-Cl···Cl-C, in **2**, reflected in its low binding energy ,Table 3. In cases of **3** and **4**, the binding energy increases from **3** (-66.23 kJ/mol, symm. code: 1-*x*,-*y*,1-*z* and -66.63 kJ/mol, symm. code: 2-*x*,-*y*,1-*z*) to **4** (-78.26 kJ/mol, symm. code: -*x*,-*y*,-*z*), Figure S1 and Table 3 (see computational details). It is to be noted that due to the relative orientation of fragments, the calculated binding energy does not represent the energy of C-X···Cl-Mn interactions individually but reflects an overall binding energy from two C-X···Cl-Mn halogen bonds and a combination of C-H···X and several H···H interactions. Although the calculated binding energies for **3** and **4** largely overestimate the C-X···Cl-Mn energies, the relative order of binding is consistent with the geometrical analysis.

Conclusions

Four new manganese(II) coordination compounds based on *N*-(4-halo)phenyl picolinamide ligands, $L^{4\text{-}F}$, $L^{4\text{-}Cl}$, $L^{4\text{-}Br}$ and $L^{4\text{-}I}$, were synthesized, characterized and their supramolecular structures were studied. An important feature in the crystal packing of these Mn(II) complexes is that adjacent discrete neutral complexes tend to link to each other through trifurcated hydrogen bonding interactions of the $_{amide}$N-H•••Cl and C-H•••Cl type. The crystal structure analyses reveal that $[MnCl_2(L^{4\text{-}F})_2]$ and $[MnCl_2(L^{4\text{-}Cl})]$ self-assemble *via* hydrogen bonding interactions, while halogen bonding interactions of the type C-X···Cl-Mn play an important role in self-assembly of both $[MnCl_2(L^{4\text{-}Br})_2]$ and $[MnCl_2(L^{4\text{-}I})_2]$ complexes. The role of these weak intermolecular interactions involving halogens were investigated using geometrical analysis, Hirshfeld surface analysis and theoretical calculations. Also, the crystal structures of these complexes are compared with those reported in the literature, namely $[MnCl_2(L^{3\text{-}Cl})_2]$, $[MnCl_2(L^{4\text{-}H})_2]$ and $[MnCl_2(L^{4\text{-}methyl})_2]$.[13] Comparing the crystal structure of $[MnCl_2(L^{4\text{-}Cl})]$ and $[MnCl_2(L^{3\text{-}Cl})_2]$ showed that there is an interplay between weak intermolecular interactions and metal coordination. This study could provide further insight into the metallosupramolecular assemblies of biologically important coordination complexes.

Experimental Section

Apparatus and reagents. All solvents such as methanol and pyridine and the chemicals, manganese (II) chlride tera hydrate, 4-chloroaniline, 4-fluoroaniline, 4-iodoaniline, 4-bromoaniline,and picolinic acid were commercially available (reagent grade) and were purchased from Merck and used without further purification. Infrared spectra (4000–400 cm^{-1}) of solid samples were taken as 1% dispersion in CsI pellets using a BOMEM - MB102 spectrometer. Melting point was obtained by a Bamstead Electrothermal type 9200 melting point apparatus and corrected.

Single crystal diffraction. For these compounds the intensity data were collected on a STOE IPDS-II or STOE-IPDS-2T

diffractometers with graphite monochromated Mo-Kα radiation, 0.71073 Å. Data were collected at a temperature of 298(2) K in an a series of ω scans in 1° oscillations and integrated using the Stoe X-AREA software package.[19] A numerical absorption correction was applied using X-RED[20] and X-SHAPE software's.[21] All the structures were solved by direct methods using SHELXS-97 and refined with full-matrix least-squares on F^2 using the SHELXL-97 program package.[22] All non-hydrogen atoms were refined anisotropically. Hydrogen atoms were added at ideal positions and constrained to ride on their parent atoms, with $U_{iso}(H) = 1.2Ueq$. All the refinements were performed using the X-STEP crystallographic software package.[23] Structural illustrations have been drawn with MERCURY windows.[24] Crystallographic details including crystal data and structure refinement are listed in Table 1.

Computational details. DFT calculations were conducted by the ORCA quantum chemistry suite.[25] The BLYP exchange-correlation functional[26] with the recent D3 empirical dispersion correction[27] (BLYP-D3) was used to evaluate the binding energies. The basis set superposition error (BSSE) is not taken into consideration because small BSSE effects are assumed to be absorbed by the D3 empirical potential.[28] The two selected fragments were cut out directly from the CIF data without optimization. An all-electron triple-zeta basis-set with a polarization functions, TZP, has been used to ascribe all the atoms. A frozen core approximation was used to treat the core electrons. Scalar relativistic effects were account for by using the zeroth-order regular approximation (ZORA).[29]

ACKNOWLEDGMENT: We would like to thank the Graduate Study Councils of Shahid Beheshti University, General Campus for financial support.

SUPPORTING INFORMATION

Electronic Supplementary Information (ESI) available: X-ray crystallographic files in CIF format for structural determination of **1**, (CCDC No. 1016027), **2**, (CCDC No. 1016026), **3**, (CCDC No. 1016023) and **4**, (CCDC No. 1016022), experimental details, selected fragments for binding energy analysis, hydrogen bond parameters for complexes **1**-**4** and Hirshfeld surface analysis details. This material is free of charge via Internet at http://pubs.rcs.org.

1. (a) S. Kitagawa, R. Kitaura, S. Noro, *Angew. Chem., Int. Ed*. 2004, 43, 2334-2375. (b) S. G. Telfer, R. Kuroda, *Coord. Chem. Rev*. 2003, 242, 33-46. (c) S. A. Barnett, N. R. Champness, *Coord. Chem. Rev*. 2003, 246, 145-168. (d) C. D. Wu, A. G. Hu, L. Zhang, W. B. Lin, *J. Am. Chem. Soc*. 2005, 127, 8940-8941. (e) B. Moulton, M. J. Zaworotko, *Chem. Rev*. 2001, 101, 1629-1658. (f) M. Hong, *Cryst. Growth Des.*, 2007, *7*, 10–14. (g) E. R. T. Tiekink, J. Zukerman-Schpector, *CrystEngComm*, 2009, 11, 1176−1186 (h) B. Cheng, A. Azhdari Tehrani, M-L. Hu, A. Morsali, *CrystEngComm*, 2014, 16, 9125–9134.
2. (a) G. R. Desiraju, Crystal Engineering. The Design of Organic Solids; Elsevier: Amsterdam, 1989. (b) P. A. Gale, J. W. Steed, "Supramolecular Chemistry, from molecules to nanomaterials", John Wiley & Sons, Chichester, 2012. (c) G. R. Desiraju, *J. Am. Chem. Soc*., 2013, 135, 9952–9967 (d) S. Das, G. W. Brudvig, R. H. Crabtree, *Chem. Commun*., 2008, 413–424. (e) H. R. Khavasi, A. Azhdari Tehrani, *CrystEngComm*, 2013, 15, 5799-5812. (f) H. R. Khavasi, M. Azizpoor Fard, *Cryst. Growth Des*., 2010, 10, 1892–1896 (g) H. R. Khavasi, A. R. Salimi, H. Eshtiagh-Hosseini, M. M. Amini, *CrystEngComm*, 2011, 13, 3710-3717.
3. (a) G. Metrangolo, G. Resnati, Halogen Bonding; Fundamentals and Applications , Springer, Berlin, 2008. (b) P. Metrangolo, F. Meyer, T. Pilati, G. Resnati, G. Terraneo, *Angew. Chem., Int. Ed.* 2008, 47, 6114−6121. (c) K. Rissanen, *CrystEngComm*, 2008, 10 1107-1113. (d) G. Metrangolo, G. Resnati, *Cryst. Growth Des*., 2012, 12, 5835–5838. (e) A. Mukherjee, S. Tothadi, G. R. Desiraju, *Acc. Chem. Res.* 2014, 47, 2514–2524 (f) B. Li, S-Q Zang, L-Y Wang, T. C.W. Mak, *Coord. Chem. Rev*. 2016, 308, 1–21
4. (a) G. Mínguez Espallargas, F. Zordan, L. Arroyo Marín, H. Adams, K. Shankland, J. van de Streek, L. Brammer, *Chem-Eur. J*., 2009, 15, 7554–7568. (b) F. F. Awwadi, R. D. Willett, B. Twamley, R. Schneider, C. Landee, *Inorg. Chem*. 2008, 47, 9327−9332. (c) F. Zordan, L. Brammer, P. Sherwood, *J. Am. Chem. Soc*., 2005, 127, 5979–5989. (d) D. A. Smith, L. Brammer, C. A. Hunter, R. N. Perutz, *J. Am. Chem. Soc.*, 2014, 136, 1288–1291 (e) H. R. Khavasi, A. Azhdari Tehrani, *Inorg. Chem*., 2013, 52, 2891–2905. (f) F. F. Awwadi, D. Taher, S. F. Haddad, M. M. Turnball, *Cryst. Growth Des*., 2014, 14, 1961–1971. (g) M. B. Andrews, C. L. Cahill, *Dalton Trans*., 2012, 41, 3911-3914. (h) K. P. Carter, C. H. F. Zulato, C. L. Cahill, *CrystEngComm*, 2014, 16, 10189-10202 . (i) J. E. Ormond-Prout, P. Smart, L. Brammer, *Cryst. Growth Des*., 2012, 12, 205–216. (j) J. S. Ovens, D. B. Leznoff, *Chem. Mater*., 2015, 27, 1465–1478 (k) S-Q Zang, Y-J Fan, J-B Li, H-W Hou, T. C. W. Mak, *Cryst. Growth Des*., 2011, 11, 3395–3405 (l) S-Q Zang, M-M Dong, Y-J Fan, H-W Hou, T. C. W. Mak, *Cryst. Growth Des.*, 2012, 12, 1239–1246
5. (a) F. Zordan, L. Brammer, *Acta Cryst*. 2004, B60, 512-519. (b) P. Smart, Á. Bejarano-Villafuerte, L. Brammer, *CrystEngComm*, 2013,15, 3151-3159 (c) P. Smart, Á. Bejarano-Villafuerte, R. M. Hendrya, L. Brammer, *CrystEngComm*, 2013, 15, 3160-3167. (d) A. Azhdari Tehrani, A. Morsali, M. Kubicki, *Dalton Trans.*, 2015, 44, 5703-5712.
6. (a) R. Bertani, P. Sgarbossa, A.Venzo, F. Lelj, M. Amati, G. Resnati, T. Pilati, P. Metrangolo, G. Terraneo, *Coord. Chem. Rev*. 2010, 254, 677−695. (b) B. Li, M-M Dong, H-T Fan, C-Q Feng, S-Q Zang, L-Y Wang, *Cryst. Growth Des*., 2014, 14, 6325–6336. (c) M. K. Panda, S. Ghosh, N. Yasuda, T. Moriwaki, G. D. Mukherjee, C. M. Reddy, P.Naumov, *Nat. Chem*. 2015, 7, 65–72.
7. (a) H. R. Khavasi, M. Mehdizadeh Barforoush, M. Azizpoor Fard, *CrystEngComm*, 2012, 14, 7236-7244 (b) H. R. Khavasi, B. Mir Mohammad Sadegh, *Dalton Trans*., 2014, 43, 5564-5573 (c) H. R. Khavasi, M. Hosseini, A. Azhdari Tehrani, S. Naderi, *CrystEngComm*, 2014, 16, 4546-4553 (d) H. R. Khavasi, A. Ghanbarpour, A. Azhdari Tehrani, *CrystEngComm*, 2014, 16, 749-752 (e) H. R. Khavasi, F. Norouzi, A. Azhdari Tehrani, *Cryst. Growth Des*., 2015, 15, 2579−2583. (f) H. R. Khavasi, M. Esmaeili, *CrystEngComm*, 2014, **16**, 8479-8485.
8. D. Domide, O. Hübner, S. Behrens, O. Walter, H. Wadepohl, E. Kaifer, H-J Himmel, *Eur. J. Inorg. Chem.* 2011, 1387–1394.
9. (a) Price, S. L.; Stone, A. J.; Lucas, J.; Rowland R. S.; Thornley, A. *J. Am. Chem. Soc.*,1994, 116, 4910-4918. (b) Awwadi, F. F.; Willett, R. D.; Peterson, K. A.; Twamley, B. *Chem. Eur. J.*, 2006, 12, 8952-8960. (c) Pedireddi, V. R.; Shekhar, D.; Reddy, Goud, B. S.; Craig, D. C.; Rae, A. D.; Desiraju, G. R. *J. Chem. Soc., Perkin Trans.* 2, 1994, 2353-2360.
10. (a) D. Braga, J. Chem. Soc., *Dalton Trans*., 2000, 3705–3713 (b) L. Brammer, Chem. Soc. Rev., 2004, 33, 476–489. (c) E. R. T. Tiekink, *Chem. Commun*., 2014, 50, 11079-11082. (d) E. Constable, G. Zhang, C. E. Housecroft, J. A. Zampese, *CrystEngComm*, 2011, 13, 6864-6870.
11. (a) C. S. Lai, S. Liu, E. R. T. Tiekink, *CrystEngComm*, 2004, 6, 221–226. (b) N.L. Kilah, M. D. Wise, P. D. Beer, Cryst. Growth Des., 2011, 11, 4565–4571. (c) R. Custelcean, T. J. Haverlock, B. A. Moyer, *Inorg. Chem*. 2006, 45, 6446-6452 (e) K. P. Cartera, C. L. Cahill, *Inorg. Chem. Front.*, 2015,2, 141-156. (f) J. de Groot, K. Gojdas, D. Unruh, T. Z. Forbes, *Cryst. Growth Des*., 2014, 14, 1357–1365. (g) L. Brammer, *Dalton Trans.*, 2003, 3145–3157.
12. (a) M. Pick, I. Roboni, J. Fridovich, J. Am. Chem. Soc., 1974, 96, 7329-7333. (b) R.J. Debus, *Biochem. Biophys. Acta*, 1992, 1102, 269-352 (c) J. B. Vincent, G. Christou, *Inorg. Chim. Acta*, 1987, 136, L41-L44.
13. (a) W. Jacob, R. Mukherjee, *J. Chem. Sci.*, 2008, 120, 447–453 (b) I. Lumb, M. S. Hundal, G. Hundal, *Inorg Chem.* 2014, 53, 7770-7779. (c) J-YQi, Y-M Li, Z-Y Zhou, C-M Che, C-H Yeung, A.S.C.Chan, *Adv.Synth.Catal.*, 2005, 347, 45-49. (d) Q. Y. Yang,

J. Y. Qi, G. Chan, Z. Y. Zhou, A.S.C. Chan, *Acta Crystallogr.,Sect.E:*2003, 59, m982-m984.
14. (a) H. R. Khavasi, K. Sasan, M. Pirouzmand, S. N. Ebrahimi, *Inorg. Chem.*, 2009, 48, 5593–5595 (b) M. Bagherzadeh, A. Ghanbarpour, H. R. Khavasi, *Catal. Commun.*, 2015, 65, 72-75.
15. (a) J. J. McKinnon, M. A. Spackman, A. S. Mitchell, *Acta Cryst.*, 2004, B60, 627–668 (b) M. A. Spackman, J. J. McKinnon, *CrystEngComm*, 2002, 4, 378–392.
16. M. J Turner, D. Jayatilaka, M. A. Spackman, CrystalExplorer 3.0; University of Western Australia: Perth, Australia, 2012.
17. (a) P. Politzer, J. S. Murray, T. Clark, *Phys. Chem. Chem. Phys.* 2010, 12, 7748−7757. (b) P. Metrangolo, H. Neukirch, T. Pilati, G. Resnati, *Acc. Chem. Res.* 2005, 38, 386−395. (c) J. S. Murray, K. E. Riley, P. Politzer, T. Clark, *Aust. J. Chem.* 2010, 63, 1598−1607.
18. S. P. Ananthavel, M. Manoharan, *Chem. Phys.* 2001, 269, 49−57.
19. Stoe & Cie, X–AREA, vesion 1.30: Program for the acquisition and analysis of data; Stoe & Cie GmbH: Darmatadt, Germany, 2005.
20. Stoe & Cie, X–RED, vesion 1.28b: Program for data reduction and absorption correction; Stoe & Cie GmbH: Darmatadt, Germany, 2005.
21. Stoe & Cie, X–SHAPE, vesion 2.05: Program for crystal optimization for numerical absorption correction; Stoe & Cie GmbH: Darmatadt, Germany, 2004.
22. G. M. Sheldrick, SHELX97. Program for crystal structure solution and refinement. University of Göttingen, Germany, 1997
23. Stoe & Cie, X-STEP32, Version 1.07b: Crystallographic package; Stoe & Cie GmbH: Darmstadt, Germany, 2000.
24. Mercury 3.1 Supplied with Cambridge Structural Database, CCDC, Cambridge, UK, 2012.
25. F. Neese, U. Becker, D. Ganyushin, D. G. Liakos, S. Kossmann, T. Petrenko, C. Riplinger and F. Wennmohs, ORCA, 2.7.0, University of Bonn, Bonn, 2009.
26. (a) A. D. Becke, *Phys. Rev.*, 1988, 38, 3098-3100 (b) C. Lee, W. Yang, R. G. Parr, Phys. Rev. B: Condens. *Matter Mater. Phys.*, 1988, 37, 785-789.
27. S. Grimme, J. Antony, S. Ehrlich, H. Krieg, *J. Chem. Phys*., 2010, 132, 154104-154119.
28. C. Fonseca Guerra, H. Zijlstra, G. Paragi, M. Bickelhaupt, *Chem – Eur. J.*, 2011, 17, 12612-12622.
29. (a) E. van Lenthe, E. J. Baerends, J. G. Snijders, *J. Chem. Phys.*, 1993, 99, 4597–4610 (b) E. van Lenthe, E. J. Baerends, J. G. Snijders, *J. Chem. Phys.*, 1994, 101, 9783–9792; (c) E. van Lenthe, van R. Leeuwen, E. J. Baerends, J. G. Snijders, *Int. J. Quantum Chem.*, 1996, 57, 281–293.

Cite this: DOI: 10.1039/x0xx00000x

The role of intermolecular interactions involving halogens in the supramolecular architecture of a series of Mn(II) coordination compounds

Hamid Reza Khavasi*, Alireza Ghanbarpour and Alireza Azhdari Tehrani

Received 00th January ????.,
Accepted 00th January ????

DOI: 10.1039/x0xx00000x

www.rsc.org/

This study reveals the role of halogen-involving interactions in structural changes of supramolecular assemblies of Manganese(II) complexes including *N*-(4-halo)phenylpicolinamide ligands.